Initial Calibration Procedure of a Six-Port Receiver System for Complex Data Reception

S. Lindner, F. Barbon, G. Vinci, R. Weigel, and A. Koelpin
Institute for Electronics Engineering, University of Erlangen-Nuremberg
91058 Erlangen, Germany
Email: {lindner, barbon, vinci, weigel, koelpin}@lfte.de

***Abstract*—In this publication a six-port receiver system for reception of modulated I/Q-data is shown. The system contains of passive six-port and diode structures to mix the signal to baseband. After digitizing the baseband voltages, a complex vector can be calculated. The binary data reconstruction is done by mapping these complex vector to the correct data symbol in the constellation diagram. Therefore, the data rate has to be reconstructed as described here. Furthermore, a simple calibration technique is explained and some measurements are taken to prove the functionality of the system and the simulation results.**

***Index Terms*—Calibration, Demodulation, Mixers, Receivers, RF signals**

I. Introduction

The six-port architecture is not a new invention, as there were already publications in the early 1970s on this topic [1]. But in former times there were many problems with it, because of the six-port disadvantages of higher computational effort in base-band signal conditioning and reconstruction [2].

Today, the requirements for high bandwidth in measurement as well as in communication systems lead to higher operating frequencies. In some cases nowadays active circuit topologies touch their limits and there is room for new solutions based on six-port architecture.

Recently, several publications present the six-port as a measurement system for phase, distance and angle-of-arrival in frequency ranges of a few GHz [3]–[5]. However, a six-port structure can also be used as a direct conversion receiver for digitally modulated RF-signals [6]–[8]. Especially, pure phase shift modulations are suitable, because of the high phase resolution capability. Certainly, also quadrature modulations can be received with a proper calibration.

The usability of a six-port for data reception will be explained in the following paragraphs. Besides a description of the investigated system, a data reconstruction and data rate recovery as well as an easy calibration technique will be shown. This calibration is necessary because of different sensitivities of the detectors, different gain of the base band amplifiers, and imbalances inside the six-port structure.

II. Receiver system

The receiving system includes a passive six-port structure, whose two input ports are connected to a continuous wave (CW) local oscillator with a frequency of 24 GHz (signal S_1) and a signal generator which is capable of generating a modulated I/Q-data signal (signal S_2), respectively.

The signal frequency of 24 GHz is used, because it is within an ISM band and therefore free to use. Surely, there are also higher and lower ISM bands, but a sixport structures makes no sense at low frequency, because of the big area consumption due to the coupler structures. On the other hand, the measuring equipment for higher frequencies like 61 GHz or above is very expensive and connecting together with measuring a system at such frequencies is difficult. For these reasons, the shown system is working at 24 GHz.

$$S_1 = A_1 \left[\cos(\omega t + \Phi_1) + \mathrm{j}\sin(\omega t + \Phi_1)\right] \quad (1)$$

$$S_2 = A_2 \left[\cos(\omega t + \Phi_2) + \mathrm{j}\sin(\omega t + \Phi_2)\right] \quad (2)$$

Inside the six-port structure these two signals are additively superimposed having discrete phase differences of $\pi/2$ and routed to the four output ports. After down-converting to baseband (by simple GaAs diode networks), the four base-band voltages B_3, B_4, B_5 and B_6 can be obtained. These voltages represent the squared six-port output signals O_3 to O_6, equivalent to the corresponding port power [9].

$$B_3 = \frac{1}{4}(A_1^2 + A_2^2 + 2A_1A_2\sin(\Phi_2 - \Phi_1)) \quad (3)$$

$$B_4 = \frac{1}{4}(A_1^2 + A_2^2 - 2A_1A_2\sin(\Phi_2 - \Phi_1)) \quad (4)$$

$$B_5 = \frac{1}{4}(A_1^2 + A_2^2 + 2A_1A_2\cos(\Phi_2 - \Phi_1)) \quad (5)$$

$$B_6 = \frac{1}{4}(A_1^2 + A_2^2 - 2A_1A_2\cos(\Phi_2 - \Phi_1)) \quad (6)$$

It is easy to understand, that (3) and (4) as well as (5) and (6) form a differential signal, respectively, with a phase difference of π between them. Furthermore, these two differential signals have a phase difference of $\pi/2$, forming a complex vector defined by its value $r = A_1A_2$ and phase $\varphi = \Phi_2 - \Phi_1$, i.e., the received and demodulated data signal. The superposition and the occurrence of the complex vector is plotted in Fig. 1.

To compensate the tolerances for the conversion characteristics of the different diodes and to use the full scale of the analog-digital-converters (ADC) controllable base-band (BB) amplifier stages are added. Between the amplifier and the digitizing stage there is an active filter with butterworth characteristics included to eliminate aliasing effects. The filters

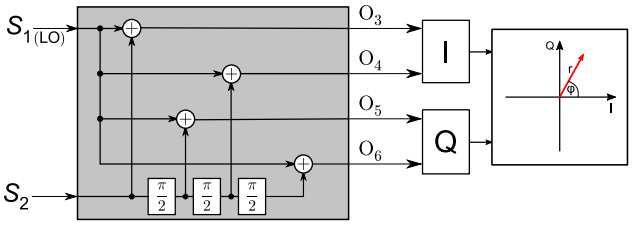

Fig. 1. Phase relationships between input and output ports of the six-port structure.

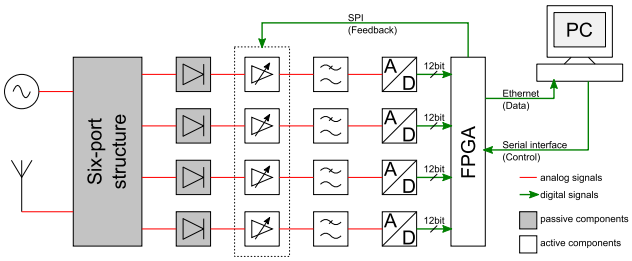

Fig. 2. Overview of acquisition system.

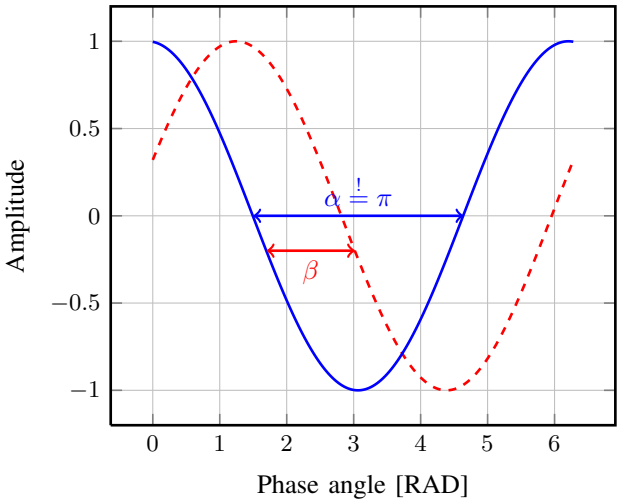

Fig. 3. Simulated calibration results of gain compensated in-phase (red, dashed) and quadrature (blue) signal components plotted over angle to determine the phase error needed for phase imbalance compensation.

are of 8th order for each channel to reach the SNR provided by the high ADC resolution at half the sampling frequency, while achieving a passband up to 50 kHz.

After digitizing the four channels with a resolution of 12 bit at a sample rate of 300 kHz, the values are transferred via an FPGA board by ethernet to a personal computer, where the further signal processing is done. This PC also controls the signal sources and configures the base band amplifiers' gain levels.

III. Initial Calibration

A simple approach for calibration is to compensate the circle deviation of a phase sweep for the received values in the complex number domain [3]. Therefore, in addition to the local oscillator, a CW input signal with a fixed variance in frequency of about 1 kHz has to be delivered. Plotting the complex values of the six-port output should result in an ideal circle, because the phase of the resulting complex vector is rotating in the constellation diagram with the difference frequency of the six-port input signals.

Calibration is then done in the complex domain with the compley vector $z = I + \mathrm{j}Q$ by calculating offset and gain correction factor K_Q to map the received signals onto the perfect circle (Fig. 4). Furthermore, the phase error ρ can be corrected to get an even better calibration result.

$$I_c = I_m - I_o \tag{7}$$

$$Q_c = K_Q \frac{Q_m - Q_o - I_c \sin\rho}{\cos\rho} \tag{8}$$

$$K_Q = \frac{max(|I_m|) - I_o}{max(|Q_m|) - Q_o} \tag{9}$$

For the first step the shown equations (7), (8) and (9) are used with $\rho = 0$. In the equations the subscript index m stands for the measured value and c stands for the corrected result, whereas the index o designates the mean value of the particular signal.

After removing offset and gain error, the phase imbalance error can be removed by calculating the correct ρ from the distance between the zero crossings of the I and Q signals plotted against time. This relation is shown in Fig. 3. The phase offset error $\rho = 0$, depending on the values of α and β, can be calculated by equation:

$$\rho = \left(\frac{1}{2} - \frac{\beta}{\alpha}\right) \cdot \pi. \tag{10}$$

That's because the zero crossings of a sine signal have the distance of π between them, while the distance of the zero crossing of sine and cosine functions of the same signal should have a difference in distance of $\pi/2$. This equation is independent from the unit of the x-axis, because the angle is normalized to the measured π by the zero crossing of one of the signals. Therefore, the calculation can be done in timedomain without projecting the phase relations of the complex vector at the timeline as done in Fig. 3 for a clearer visualization.

Fig. 4 shows the results of the described calibration routine. The uncorrected signal, the perfect reference circle, and the two calibration stages are displayed in different colors.

This calibration algorithm is pretty simple and it is only necessary to calculate the four calibration parameters I_o, Q_o, K_Q and ρ. It should be mentioned, that the calibration is done at only one power level. Therefore, it is mainly useful for modulation types with fixed amplitude or pure phase measurements. Furthermore, this routine is used for initial calibration after the six-port system has been manufactured. For in-situ calibration there are more suitable calibration procedures.

After removing gain and phase imbalances with this procedure it is additionally necessary to eliminate the phase offset between local oscillator and the received signal. This is very

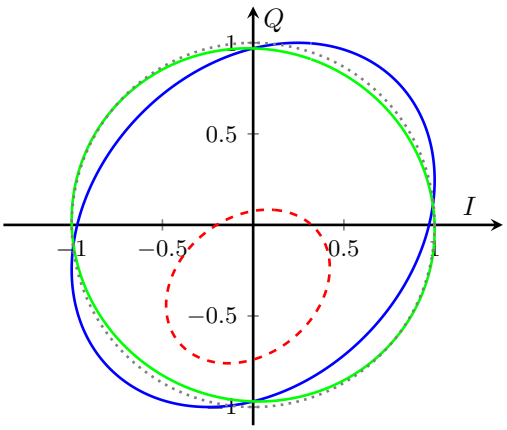

Fig. 4. Simulated calibration results: The figure illustrates an original measured data signal (red, dashed) with random variations in gain and phase. Furthermore, the corrected results from the given equations with $\rho = 0$ (blue) and with the additional computed correct $\rho = 0.085\pi$ (green) are plotted. A perfect circle is shown (dotted) as reference.

important to get the correct constellation diagram. This error leads to a rotated constellation diagram and can be removed by calculating the angle error and rotating back the complex vector by a simple complex multiplication. The procedure for getting this angle depends on the used modulation. To avoid a wrong rotation a start sequence or a pilot tone should be used in the transmitted signal. The shown setup is using an known start sequence to avoid an wrong rotation.

IV. Data Reconstruction

The transmitted data can easily be reconstructed by using a constellation diagram and mapping the calculated phase and amplitude values of the complex vector from the sampling points to the appropriate symbol.

The complex vector z with its in-phase I and quadrature Q component can directly be extracted from the baseband-voltages:

$$\Im\{z\} : Q = B_3 - B_4 \quad (11)$$

$$\Re\{z\} : I = B_5 - B_6 \quad (12)$$

$$z = I + \mathrm{j}Q \quad (13)$$

$$= A_1 A_2 \left(\cos\varphi + \mathrm{j}\sin\varphi\right) \quad (14)$$

$$= A_1 A_2 e^{\mathrm{j}\varphi} \text{ with } \varphi = \Phi_2 - \Phi_1. \quad (15)$$

It can be seen, that the recovered complex vector z depends, besides the received signal with the power A_2 and the phase information Φ_2, also on the power A_1 and phase Φ_1 of the local oscillator. Therefore, it is important to use a source with a constant, regulated phase and output power. In that case the influence can easily removed by substracting the phase and dividing throught the power.

The signal can now be plotted in a constellation diagram. To reconstruct the analog signal, it is necessary to know the symbol rate and the beginning of at least one symbol to get the discrete points at which the data has to be read. This information can be recovered from the signal in time domain

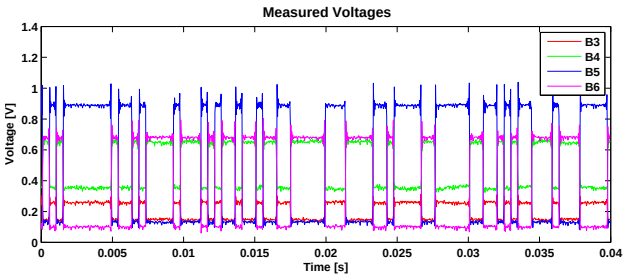

Fig. 5. Digitized uncalibrated voltages measured with the ADC.

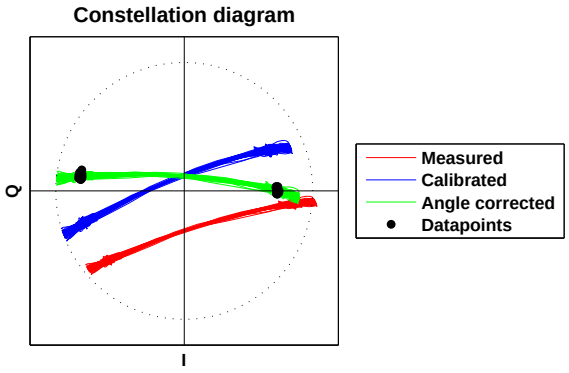

Fig. 6. Constellation diagram with a demodulated bi-phase-shift-keying modulation. Among the measured values, also the calibrated and angle-corrected values with the calculated data points are plotted.

by measuring the time between following bit changes, and assuming that the shortest time difference is the duration of one bit. This is only possible if enough bit changes occur. Therefore, an adequate start sequence at the beginning of the data transmission should be inserted, or a channel encoding such as a Manchester code should be used.

V. Measurements

The measurements are conducted with a carrier frequency of 24 GHz and a data rate of 2 kSa/s. As modulation type for the reconstruction algorithm binary phase-shift keying (BPSK) was used because regeneration of data rate is simple in this case. In Fig. 5 the measured six-port output voltages measured by the ADC-Board are displayed. These values are uncompensated, having an offset and gain error. The complex data signal, calculated from these values is shown in a constellation diagram in Fig. 6. Furthermore, this figure shows the calibrated and angle corrected version of the complex vector and the recovered sampling points. The processed values can be seen in Fig. 7, where the calibrated and normalized time domain signal of the data stream are shown.

Data reconstruction can now be done by reading out the time domain signal at the data points or calculating the angle of the complex vector at these points. With these values a look-up-table can be used to get the correct symbol, or in this case the bit.

The system is also capable of higher types of modulation.

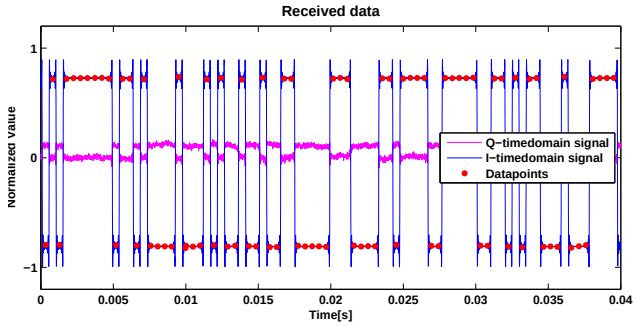

Fig. 7. Time domain measurements of the in-phase and quadrature components, with marked sample points, at which the data are used to reconstruct the sent symbol.

Several schemes have been acquired and their constellation diagrams are plotted in Fig. 8. The data points are clearly visible. Therefore, a reconstruction should be also possible. At QAM-16 there is a noticeable distortion, that can be traced back to the used calibration at only one power level. Expanding of the calibration procedure to different power levels will solve this problem.

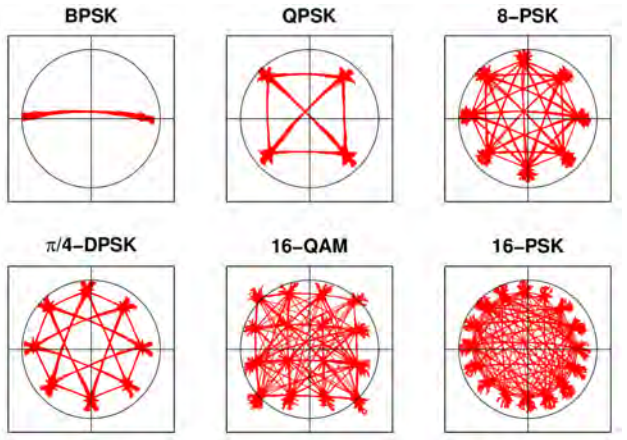

Fig. 8. Constellation diagrams of several types of digital modulations, acquired with the presented six-port system.

VI. Conclusion

The system presented in this publication shows the functionality of the six-port architecture as a receiver for complex modulated digital data. Constellation diagrams of various types of modulations were acquired, while signal reconstruction and data clock recovery was exemplary shown with the help of BPSK modulated signal for a data rate of 2 kSa/s.

Furthermore, an easy, but sufficient initial calibration technique for this type of receiver has been presented and validated by simulations and measurements.

References

[1] C. Hoer, "The six-port coupler: a new approach to measuring voltage, current, power, impedance, and phase," *Instrumentation and Measurement, IEEE Transactions on*, vol. IM-21, no. 4, pp. 466–470, November 1972.

[2] F. M. Ghannouchi and A. Mohammadi, *The Six-Port Technique*. Artech House, 2009.

[3] B. Laemmle, G. Vinci, L. Maurer, R. Weigel, and A. Koelpin, "An integrated 77-ghz six-port receiver front-end for angle-of-arrival detection," in *Bipolar/BiCMOS Circuits and Technology Meeting (BCTM), 2011 IEEE*, oct. 2011, pp. 219 –222.

[4] G. Vinci, A. Koelpin, F. Barbon, and R. Weigel, "Six-port-based direction-of-arrival detection system," in *Proc. Asia-Pacific Microwave Conference APMC 2010*, 2010, eingereicht.

[5] G. Vinci, F. Barbon, R. Weigel, and A. Koelpin, "A novel, wide angle, high resolution direction-of-arrival detector," in *Radar Conference (EuRAD), 2011 European*, oct. 2011, pp. 265 –268.

[6] S. M. Winter, A. Koelpin, and R. Weigel, "Six-port receiver analog front-end: Multilayer design and system simulation," vol. 55, no. 3, pp. 254–258, March 2008.

[7] M. Mohajer and A. Mohammadi, "A novel architecture for six-port direct conversion receiver," in *Personal, Indoor and Mobile Radio Communications, 2004. PIMRC 2004. 15th IEEE International Symposium on*, vol. 4, 5-8 Sept. 2004, pp. 2705–2709Vol.4.

[8] J. Hyyrylainen, L. Bogod, S. Kangasmaa, H. Scheck, and T. Ylamurto, "Six-port direct conversion receiver," in *Microwave Conference and Exhibition, 27th European*, Sep. 8-12, 1997, pp. 341–346.

[9] S. Winter, H. Ehm, A. Koelpin, and R. Weigel, "Diode power detector dc operating point in six-port communications receivers," in *Proc. European Microwave Conference*, Oct. 9–12 2007, pp. 795–798.